Long-Term Evolution of Near-Geostationary Orbits

Jozef C. Van der Ha*
European Space Operations Center, Darmstadt, Federal Republic of Germany

A model for the long-term evolution of free-drifting near-geostationary satellite orbits is presented. A first-order analytical averaging transformation is applied to the perturbation equations in order to eliminate the short-term (with period of order of one day) variations of the orbital elements. The model includes lunisolar gravitational forces up to the second parallactic term of the moon, zonal and tesseral harmonics of the Earth's potential field up to the fourth degree, as well as the solar radiation force. The algebraic computations have been carried out by an automated Poisson series manipulation. Extremely compact expressions could be established after manually recombining the computer-generated results in terms of a few well-selected parameters. The results obtained are of particular interest for predicting the motion of geostationary spacecraft after their useful lifetime has expired and stationkeeping maneuvers are no longer executed. The validity of the model presented has been evaluated by a comparison with numerical results obtained for the European Space Agency's GEOS-2 satellite, which is at present orbiting about 260 km above geostationary altitude.

Nomenclature

a = semimajor axis
$a_j, b_{jk}, c_{jk\ell}, d_{jk\ell m}$ = coefficients defined in Eqs. (16)
A = effective illuminated satellite area
$[A]$ = inclination matrix, Eq. (14)
A_{jc}, A_{js} = elements of matrix $[A]$, Eq. (14)
c_σ = auxiliary parameter, $(1+\sigma)^{-1/2}$
C, S = auxiliary parameters, Eqs. (17)
$C_{\ell mp}, S_{\ell mp}$ = auxiliary functions, Eqs. (31)
e = eccentricity vector
f, g = nonsingular eccentricity elements, Eqs. (1)
$f(\chi)$ = auxiliary function, Eq. (48)
$F_{\ell mp}$ = Kaula's inclination functions (Ref. 16)
h, k = nonsingular inclination elements, Eqs. (1)
$H_{\ell mp}, K_{\ell mp}$ = nonsingular inclination functions, Eqs. (32)
i = inclination
J_n = zonal harmonic coefficients
$J_{\ell m}$ = tesseral harmonic coefficients
L = true longitude, $\omega+\Omega+\theta$
m = mass of satellite
M = mean anomaly
n = mean orbital rate
n_s = Earth's rotation rate, 7.292116×10^{-5} rad/s
$\bar{n}_s$ = reference rotation rate, Eq. (46)
p' = parallactic factor, Eqs. (11)
P_j = jth Legendre polynomial
$P_{\ell m}$ = associated Legendre functions of first kind
r = radial position vector of satellite
r_s = reference geostationary altitude, 42164.2 km
R = general disturbing function
R_E = Earth's equatorial radius, 6378.14 km
S' = solar radiation pressure, 4.51×10^{-6} Pa
t = time
u = unit vector from Earth to satellite with components u_j
u' = unit vector from Earth to third body with components u'_j
$\bar{u}, u_c^k, u_s^k$ = Fourier coefficients of u, Eqs. (13)
X = auxiliary parameter, $1+h^2+k^2$
α = right ascension
$\beta_{\ell mp}, \gamma_{\ell mp}$ = auxiliary tesseral angular coefficients, Eqs. (30) and (A2)
δ = geographical latitude
ϵ' = third-body perturbation parameter, Eqs. (11)
ϵ_n = zonal perturbation parameters, Eqs. (24)
$\epsilon_{\ell m}$ = tesseral pertubation parameters, Table 1
ϵ_{SR} = solar radiation perturbation parameter, Eq. (38)
θ = true anomaly
λ = geographical longitude
Λ = mean longitude, Eq. (2)
$\lambda_{\ell m}$ = tesseral angular coefficients, Table 1
μ = Earth's gravitational parameter, $3.98601\times10^{14}\times10^{14}$ m^3/s^2
ξ' = auxiliary parameter, $u\cdot u'$
σ = normalized semimajor axis deviation, Eq. (4)
τ = reflectivity parameter in solar radiation model
ϕ = argument of latitude, $\omega+\theta$
χ = drift angle, Eq. (6)
ψ = auxiliary drift angle, Eq. (5)
ω = argument of perigee
Ω = right ascension of ascending node
$\langle\ \rangle$ = secular part of function enclosed

Subscripts

s = nominal (i.e., on-station or reference) values
SR = solar radiation
tess = tesseral
zon = zonal
0 = initial conditions

Superscripts

$(\ )'$ = third body
$(\dot{})$ = derivative with respect to time

Introduction

THE evolution of a geostationary orbit has been of great interest over the past 20 years and at present its behavior is well known. The Earth's oblateness together with the lunisolar gravitational attraction cause the orbit pole to precess along a full angle cone of about 14.6 deg over a period of some 52 years. A qualitative explanation of this precessional motion can be found in Allen and Cook.[1]

A second important feature of the free-drift orbit evolution is the periodic longitude drift motion coupled with semimajor

Received March 4, 1985.
*Senior Analyst. Member AIAA.

axis oscillations. These long-period effects (with a period of more than two years) are caused by the ellipticity of the Earth's equator. Although the maximum variation in the equator's cross section is less than 100 m, this effect is capable of inducing longitude oscillations up to 180 deg amplitude for the right initial satellite position. In that case, the corresponding semimajor axis oscillation reaches a maximum value of about 33 km. These effects are described in detail by Allen[2] and Blitzer,[3] for instance.

The third characteristic of the long-term free-drift motion refers to the eccentricity vector behavior. For present-day communications satellites with an area/mass ratio in the order of 0.02 m^2 /kg, the main perturbing effect is provided by solar radiation forces, with the moon's parallactic influence as a secondary effect. The resulting motion of the eccentricity vector consists of circular loops of one-year duration with curly waves due to the moon's effect superimposed on it.

Approximate analytical theories describing the long-term geostationary orbit evolution have been developed by, for instance, Flury,[4] Graf,[5] and Richardson.[6] Other theories (e.g., Kamel[7]) are valid particularly for station-kept satellites with the property that deviations from the reference position are small. An outline of stationkeeping strategies and the operational aspects of geostationary satellite support is given by Soop.[8]

Recently, interest in the long-term geostationary orbit evolution has been spawned by the enormous expansion in the geostationary satellite services required. Problems related to the overfilling (such as collision risks) of the geostationary ring will become more and more serious in the near future.[9] Therefore, strong recommendations are being made for the deorbiting of satellites after their useful lifetime has expired. An account of the deorbiting strategy and operations at the time of the European Space Agency's (ESA) GEOS-2 orbit raising can be found in the literature.[10]

The present paper aims at providing a complete model for the long-term free-drift evolution of a near-geostationary orbit. A first-order analytical averaging transformation is implemented that results in a saving in numerical calculation time by a factor of 20. By means of an automated Poisson series manipulator,[11] it is possible to construct the secular contributions of the various disturbing functions in a relatively reliable and quick manner. It is striking that extremely compact expressions for the secular part of the lunisolar perturbations can be established after a manual recombination of the computer-generated results. Zonal and tesseral gravitational harmonics of the Earth are included up to the fourth degree and analyzed as to their secular contributions. Solar radiation forces are modeled by means of constant material parameters.

The theory presented has been used in the assessment of collision probabilities by predicting the long-term motion of abandoned geostationary satellites. The model is also useful in orbit predictions for satellites after their removal from geostationary orbit. The results have been compared with those from a numerical theory that includes all of the short-periodic perturbations using the orbit elements of ESA's GEOS-2 satellite. This spacecraft was injected into an orbit about 260 km above the geostationary altitude in early 1984.[10]

Equations of Perturbed Motion

Nonsingular Elements

A near-geostationary orbit is characterized by near-zero eccentricity and near-zero inclination. In order to avoid the singularities in the rates of change of the lines of apsides (for $e=0$) and nodes (for $i=0$), a set of nonsingular equinoctial elements[12] is adopted, as follows

$$f=e\cos(\omega+\Omega), \qquad g=e\sin(\omega+\Omega)$$

$$h=\tan(i/2)\cos\Omega, \qquad k=\tan(i/2)\sin\Omega \tag{1}$$

From Fig. 1, it can be seen that f and g represent the broken-angle projections of the eccentricity vector $\boldsymbol{e}$ (pointing to the instantaneous perigee position) upon the equatorial X and Y axes, which are taken to be inertial. The elements h and k are related to the projections of the orbit's polar vector (along the instantaneous orbit angular momentum vector) upon the same axes. The mean longitude Λ will be employed as the corresponding fast angular variable,

$$\Lambda=M+\omega+\Omega \tag{2}$$

representing the broken-angle "mean position" of the satellite relative to the X axis.

The perturbation equations for the chosen set of orbital elements (f,g,h,k,Λ,a) can be derived from the familiar results for the classical orbital elements, for instance, by application of Campbell's formula,[13]

$$\dot{f}=-\frac{s}{na^2}R_g-\frac{gX}{2na^2s}\{hR_h+kR_k\}-\frac{fs}{na^2(1+s)}R_\Lambda$$

$$\dot{g}=\frac{s}{na^2}R_f+\frac{fX}{2na^2s}\{hR_h+kR_k\}-\frac{gs}{na^2(1+s)}R_\Lambda$$

$$\dot{h}=\frac{hX}{2na^2s}\{gR_f-fR_g-R_\Lambda\}-\frac{X^2}{4na^2s}R_k$$

$$\dot{k}=\frac{kX}{2na^2s}\{gR_f-fR_g-R_\Lambda\}+\frac{X^2}{4na^2s}R_h$$

$$\dot{\Lambda}=n+\frac{s}{na^2(1+s)}\{fR_f+gR_g\}$$

$$+\frac{X}{2na^2s}\{hR_h+kR_k\}-\frac{2na^2}{\mu}R_a$$

$$\dot{a}=\frac{2na^2}{\mu}R_\Lambda \tag{3}$$

where derivatives of the disturbing function R with respect to the adopted elements are indicated by subscripts, e.g., $R_f=\partial R/\partial f$.

Since the relative semimajor axis variations turn out to be small, it is useful to introduce the normalized deviation

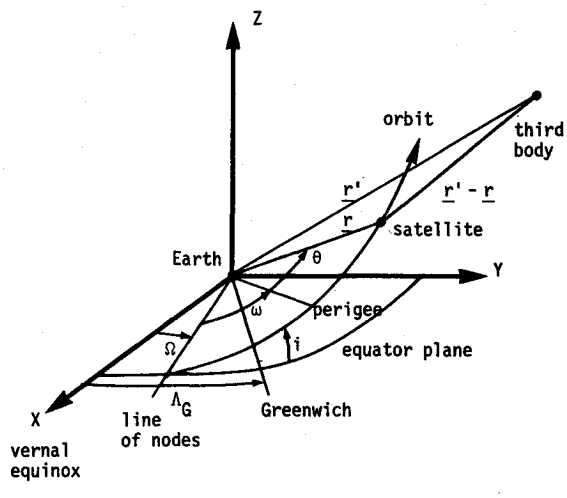

Fig. 1 Orbit geometry for near-geostationary satellite.

relative to a constant reference radius r_s,

$$\sigma = (a - r_s)/r_s \tag{4}$$

As a reference radius, the unperturbed approximation of the geostationary altitude, i.e., $r_s = \mu/n_s)^{1/3} = 42164.2$ km. It should be recalled that the Earth's oblateness introduces an extra gravitational pull on an equatorial orbit, so that the actual geostationary altitude and semimajor axis are higher than r_s.

It is convenient to write the mean longitude's rate of change as $n + \dot{\psi}$ with ψ as a slow variable whose rate of change is defined by the equation for $\dot{\Lambda}$ in Eq. (3). The drift rate $\dot{\chi}$ relative to the Earth's rotation rate can be expressed as

$$\dot{\chi} = \dot{\Lambda} - n_s = n_s(c_\sigma^3 - 1) + \dot{\psi} \tag{5}$$

To keep track of the drift angle itself, one may write

$$\chi(t) = n_s \eta(t) + \psi(t), \tag{6}$$

with $\dot{\eta} = c_\sigma^3 - 1$. The equation for $\dot{\eta}$ can be considered as an extension of the system of perturbation equations in Eq. (3).

First-Order Averaged Equations

The disturbing function R for the relevant perturbing forces must be expressed in the selected nonsingular elements. It will take the form of a Poisson series with Λ as the angular fast variable appearing only within the arguments of sine and cosine terms. After substituting the derivatives of R in Eqs. (3), the short-periodic terms (2π periodic in Λ) can be eliminated by applying a near-identity transformation from instantaneous osculating to mean elements. The system of equations for the mean elements is obtained by averaging the right-hand sides of Eqs. (3) over one revolution of Λ. Particular care must be exercised in the analysis of the tesserral harmonics of the geopotential where a close synchronism (i.e., near resonance) exists between the satellite's mean angular rate and the Earth's rotation rate. This implies that also the Greenwich hour angle ($n_s t$ + const) must be treated as a fast variable. In the present model, this will be accomplished by expressing it in terms of $(\Lambda - \chi)$ by means of Eqs. (5) before application of the averaging operation.

It is evident that, for nonresonance perturbations, all terms R_Λ in Eqs. (3) will vanish after averaging because Λ occurs only in trigonometric arguments. For the same reason, one can replace the derivative R_Λ in Eqs. (3) by R_ψ or R_χ [cf., Eqs. (5) and (6)] in the case of resonance perturbations. These observations allow us to perform the averaging on the disturbing function itself before evaluating its derivatives with respect to the elements.

A final simplification is introduced by taking advantage of the fact that the eccentricity is small (at most of order 10^{-3}) so that terms of order e^2 may be neglected. Since the inclination of an uncontrolled geostationary orbit grows up to about 15 deg, the inclination will be carried along in an exact manner. For orbits sufficiently close to geostationary altitude, it would be legitimate to use a linear expansion of c_σ for small σ. In general, however, the exact form should be used.

The new disturbing function R is defined as

$$R = 86400\langle R\rangle/(n_s r_s^2) = 6.664575 \times 10^{-7}\langle R\rangle \tag{7}$$

in units of radians per day; $\langle R\rangle$ refers to the secular part (after averaging over Λ) of the original R in Eqs. (3). The system of averaged equations derived from Eqs. (3) is now as follows:

$$\begin{aligned}
\dot{f} &= -(c_\sigma/2)\{2R_g + fR_\psi + gX(hR_h + kR_k)\} \\
\dot{g} &= (c_\sigma/2)\{2R_f - gR_\psi + fX(hR_h + kR_k)\} \\
\dot{h} &= (c_\sigma/4)X\{2h(gR_f - fR_g - R_\psi) - XR_k\} \\
\dot{k} &= (c_\sigma/4)X\{2k(gR_f - fR_g - R_\psi) + XR_h\} \\
\dot{\psi} &= (c_\sigma/2)\{fR_f + gR_g + X(hR_h + kR_k)\} - (2/c_\sigma)R_\sigma \\
\dot{\sigma} &= (2/c_\sigma)R_\psi
\end{aligned} \tag{8}$$

The independent variable time is now counted in days rather than seconds. Because of the differentiations in Eqs. (8), it is necessary to develop the disturbing function R up to second-order eccentricity terms.

Averaged Disturbing Functions

The averaged expressions for the disturbing functions corresponding to the relevant near-geostationary perturbing forces will be developed successively.

Lunisolar Perturbations

The lunisolar perturbing force originates from the differential gravitational attraction of the satellite and the Earth by the respective third body. The disturbing function may be expressed as (cf., Fig. 1)

$$R' = \mu'\{1/|r' - r| - (r \cdot r')/(r')^3\} \tag{9}$$

After expansion of this expression in terms of powers of (r/r'), the effective averaged disturbing function for a near-geostationary orbit may be written in the form

$$R' = \epsilon' \sum_{j=2}^{\infty} \{(p')^{j-2}(a'/r')^{j+1}(1+\sigma)^j < (r/a)^j P_j(\xi') > \} \tag{10}$$

where

$$\begin{aligned}
\epsilon' &= 86400\mu'/[n_s(a')^2] = 4.69673 \times 10^{-5} \text{rad/day (sun)} \\
&= 1.02272 \times 10^{-4} \text{ rad/day (moon)} \\
p' &= r_s/a' = 2.81850 \times 10^{-4} \text{ (sun)} \\
&= 0.109689 \text{ (moon)}
\end{aligned} \tag{11}$$

The so-called parallactic term p' for the sun will be neglected, but up to second-order parallactic terms for the moon will be taken into account.

The satellite's mean longitude Λ is contained in the terms r/a and in P_j through u. By means of automated Poisson series manipulations based on the transformation from true anomaly to mean longitude, one can establish the following Fourier expansions:

$$u = \bar{u} + \sum_{k=1}^{3} \{u_c^k \cos(k\Lambda) + u_s^k \sin(k\Lambda)\} + \mathcal{O}(e^3) \tag{12}$$

with

$$\begin{aligned}
\bar{u} &= -[A](f,g)^T \\
u_c^1 &= [A]\{1 - (9f^2 + 7g^2)/8, -fg/4\}^T \\
u_c^2 &= [A](f, -g)^T \\
u_c^3 &= [A]\{9(f^2 - g^2)/8, -9fg/4\}^T \\
u_s^1 &= [A]\{-fg/4, 1 - (7f^2 + 9g^2)/8\}^T \\
u_s^2 &= [A](g,f)^T \\
u_s^3 &= [A]\{9fg/4, 9(f^2 - g^2)/8\}T
\end{aligned} \tag{13}$$

and the "inclination matrix"

$$[A]=\begin{bmatrix} A_{1_c} & A_{1_s} \\ A_{2_c} & A_{2_s} \\ A_{3_c} & A_{3_s} \end{bmatrix}=\frac{1}{X}\begin{bmatrix} X-2k^2 & 2hk \\ 2hk & X-2h^2 \\ -2k & 2h \end{bmatrix} \tag{14}$$

In fact, these expressions can be readily carried to higher order in f and g, but only up to second-order terms are needed here.

Subsequently, the terms $(r/a)^j$ for $j=2,3,4$ are expressed in their Poisson series development in terms of Λ. These will be needed for calculating the products of $(r/a)^j$ with the Legendre polynomials $P_j(\xi')$ for $j=2,3,4$. In explicit form, one may write these products as

$$(r/a)^2P_2(\xi')=-(r/a)^2/2+\sum_{j,k=1}^{3}\{b_{jk}u_j'u_k'\}$$

$$(r/a)^3P_3(\xi')=-\sum_{j=1}^{3}a_ju_j'+\sum_{j,k,\ell=1}^{3}\{c_{jk\ell}u_j'u_k'u_\ell'\}$$

$$(r/a)^4P_4(\xi')=\frac{3}{8}-\frac{5}{2}\sum_{j,k=1}^{3}\{b_{jk}u_j'u_k'\}+\sum_{j,k,\ell,m=1}^{3}\{d_{jk\ell m}u_j'u_k'u_\ell'u_m'\} \tag{15}$$

The coefficients appearing here consist of products of $(r/a)^j$ and inertial components of the vector $\boldsymbol{u}$

$$a_j=3/2(r/a)^3u_j \qquad (j=1,2,3)$$

$$b_{jk}=3/2(r/a)^2u_ju_k \qquad (j,k=1,2,3)$$

$$c_{jk\ell}=5/2(r/a)^3u_ju_ku_\ell \qquad (j,k,\ell=1,2,3)$$

$$d_{jk\ell m}=35/8(r/a)^4u_ju_ku_\ell u_m \qquad (j,k,\ell,m=1,2,3) \tag{16}$$

It may be noted that these four entries contain 3, 9, 27, and 81 terms, respectively, of which 3, 6, 10, and 15 are different. These terms have been evaluated by automated Poisson series multiplications up to second-order eccentricity terms. Since here the attention is focused on obtaining the average of the disturbing function, only the secular (i.e., nonharmonic) parts of Eqs. (15) are of interest. It is remarkable that the lengthy computer-generated secular terms can be rearranged in extremely compact forms when introducing the parameters

$$C=\sum_{j=1}^{3}(A_{j_c}u_j'),\quad S=\sum_{j=1}^{3}(A_{j_s}u_j') \tag{17}$$

These parameters are of a hybrid nature, i.e., they contain the elements h and k belonging to the satellite orbit as well as the unit vector components u_j' of the third body. The final result for the secular part contained in the main term $(j=2)$ of the disturbing function becomes

$$\langle(r/a)^2P_2(\xi')\rangle=-\tfrac{1}{2}+\tfrac{3}{4}(C^2+S^2)-\tfrac{3}{4}e^2+3(fC+gS)^2-\tfrac{3}{4}(fS-gC)^2+\mathcal{O}(e^4) \tag{18}$$

The first parallactic term $(j=3)$ contains the secular part

$$\langle(r/a)^3P_3(\xi')\rangle=(15/4)(fC+gS)[1-(5/4)(C^2+S^2)]+\sigma(e^3) \tag{19}$$

Similarly, the second parallactic term $(j=4)$ possesses the secular contribution

$$\langle(r/a)^4P_4(\xi')\rangle=3/8-(15/8)(C^2+S^2)+(105/64)(C^2+S^2)^2+\mathcal{O}(e^2) \tag{20}$$

where the e^2 terms have been neglected, since they would be of a similar order as e^3 terms in the moon's main term due to the multiplication by the factor $(p')^2$. It is of interest to note that the contribution of all $d_{jk\ell m}$ terms of Eqs. (15) is incorporated in the $(C^2+S^2)^2$ term obtained after recombination of 66 separate terms in the computer-generated results.

After substitution of Eqs. (18-20) into the disturbing function of Eq. (10), the derivatives with respect ot the elements as needed in Eq. (8) can readily be evaluated.[14] It is important to note that during all averaging operations the slowly varying third-body parameters are considered to be independent of Λ. In particular, this means that the moon's motion of about 13 deg per day is replaced by a representative constant position for each satellite revolution.

The sun's and moon's ephemeris enter the disturbing function via ξ' and $(a'/r')^j$, cf. Eq. (10). An analytical ephemeris has been constructed with the objective of providing at least three accurate digits in all third-body positions over a 20 year interval. The moon's apsidal (8.85 year period) and nodal (18.6 year period) precession rates are incorporated in the model by a linear function of time. The reference ephemeris values for the third-body elements and rates are evaluated at the midpoint of the interval considered. The inertial reference frame to which all satellite and third-body position vectors are referred corresponds to the mean equinox-of-date frame at this reference time. The precession of the equinoxes (26,000 year period) leads to a discrepancy between the adopted and actual mean equinox-of-date frames of about 0.13 deg at the extremes of a 20 year period.

Gravity Field Zonal Harmonics

Because of the Earth's nonspherical mass distribution, its potential field contains perturbing terms that are usually classified as zonal harmonics (axisymmetric contributions) and tesseral harmonics (longitude-dependent terms).

The zonal harmonics form a conservative potential field and are described by the disturbing function,

$$R_{\text{zon}}=-\left(\frac{\mu}{r}\right)\sum_{n=2}^{\infty}\left\{J_n\left(\frac{R_E}{r}\right)^nP_n(\sin\delta)\right\} \tag{21}$$

For a near-geostationary orbit, one obtains in units of radians/day,

$$R_{\text{zon}}=-\sum_{n=2}^{\infty}\{\epsilon_n(1+\sigma)^{-n-1}\langle(a/r)^{n+1}P_n(u_3)\rangle\} \tag{22}$$

where

$$\epsilon_n=86400\,n_s(R_E/r_s)^nJ_n \tag{23}$$

On the basis of GEM 8 constants,[15] one finds

$$\epsilon_2=1.560798\times10^{-4}$$

$$\epsilon_3=-5.53\times10^{-8},\qquad \epsilon_4=-5.3\times10^{-9} \tag{24}$$

Still higher coefficients are neglected in the present model. The secular part of the zonal disturbing function in Eq. (22) is evaluated by automated Poisson series multiplication of terms $(a/r)^{n+1}$ with $P_n(u_3)$ using the series of r and $\boldsymbol{u}$ as functions of the mean longitude,

$$\langle(a/r)^3P_2(u_3)\rangle=-\tfrac{1}{2}(1+3e^2/2)(1-6/X+6/X^2)+\mathcal{O}(e^4)$$

$$\langle a/r)^4P_3(u_3)\rangle=3(fk-gh)(1-5/X+5/X^2)/X+\sigma(e^3)$$

$$\langle(a/r)^5P_4(u_3)\rangle=(3/8)(1+5e^2)(1-20/X+90/X^2-140/X^3+70/x^4) \tag{25}$$

where terms of order $\epsilon_4 e^2 i^2$ are neglected since they are of similar magnitude as the $\epsilon_3 e^2$ terms. The derivatives of the disturbing function can be constructed without difficulty.[14]

It may be recalled that the principal effect of the zonal harmonics on a near-geostationary orbit consists of the precession and regression of the lines of apsides and nodes, respectively, with periods of about 74 and 37 years. Also, the drift rate is affected by the euqatorial bulge.

Gravity Field Tesseral Harmonics

The longitude-dependent or tesseral harmonics of the Earth's potential field induce a change in orbital energy with a rate depending on the satellite's longitudinal position. These energy changes are connected to variations in semimajor axis and mean motion that may lead to substantial drifts in the satellite's longitudinal position relative to the Earth.

The tesseral disturbing function is given by:

$$R_{\text{tess}} = \left(\frac{\mu}{r}\right) \sum_{\ell=2}^{\infty} \sum_{m=1}^{\ell} \left\{ J_{\ell m} \left(\frac{R_E}{r}\right)^{\ell} P_{\ell m}(\sin\delta) \cos[m(\lambda - \lambda_m)] \right\} \tag{26}$$

In the near-geostationary form the averaged disturbing function in units of radians/day can be expressed as

$$R_{\text{tess}} = \sum_{\ell=2}^{\infty} \sum_{m=1}^{\ell} \left\{ \epsilon_{\ell m} (1+\sigma)^{-\ell-1} \left\langle \left(\frac{a}{r}\right)^{\ell+1} P_{\ell m}(u_3) \cos[m(\lambda - \lambda_{\ell m})] \right\rangle \right\} \tag{27}$$

where

$$\epsilon_{\ell m} = 86400 n_s (R_E/r_s)^{\ell} J_{\ell m} \tag{28}$$

Table 1 summaries the tesseral coefficients based on GEM 8 values.[15] Higher terms are of smaller magnitude and are ignored here.

The evaluation of the secular contribution of Eq. (27) is based on Kaula's approach,[16] which leads to the identity

$$P_{\ell m}(u_3)\cos[m(\lambda - \lambda_{\ell m})] = \sum_{p=0}^{\ell} F_{\ell m p} \begin{Bmatrix} \cos \\ \sin \end{Bmatrix} [(\ell - 2p)L - m\Lambda + \beta_{\ell m p}] \quad \text{for } (\ell - m) = \begin{Bmatrix} \text{even} \\ \text{odd} \end{Bmatrix} \tag{29}$$

The phase angle $\beta_{\ell m p}$ (cf. Fig. 2) is defined as

$$\beta_{\ell m p} = m(\chi + \lambda_s - \lambda_{\ell m}) - (\ell - 2p - m)\Omega \tag{30}$$

It must be recognized that the argument of the trigonometric function in Eq. (29) contains two fast variables, namely L and Λ, whereas $\beta_{\ell m p}$ is a slow variable. In order to lump all fast-varying terms in Eqs. (27) together, one introduces the auxiliary functions

$$\begin{Bmatrix} C_{\ell m p} \\ S_{\ell m p} \end{Bmatrix} = \left(\frac{a}{r}\right)^{\ell+1} \begin{Bmatrix} \cos \\ \sin \end{Bmatrix} [(\ell - 2p)L - m\Lambda] \tag{31}$$

Furthermore, the nonsingular equivalents of the Kaula inclination functions are defined as

$$H_{\ell m p} = F_{\ell m p} \cos\beta_{\ell m p}; \quad K_{\ell m p} = F_{\ell m p} \sin\beta_{\ell m p} \tag{32}$$

These functions can be evaluated explicitly using Kaula's tabulated results[16] for $F_{\ell m p}$. The results required here for ℓ, m up to 4,2 are summarized in the Appendix.

Table 1 Summary of $\lambda_{\ell m}$ and $\epsilon_{\lambda m}$ based on GEM 8

ℓ	m	$\lambda_{\ell m}$, deg	$\epsilon_{\ell m} \times 10^6$
2	2	−14.91	0.2611
3	1	7.00	0.0482
3	2	−17.39	0.0081
3	3	21.06	0.0048
4	1	−138.60	0.0022
4	2	31.22	0.0006
4	3	−3.76	0.0002
4	4	30.67	0.0000

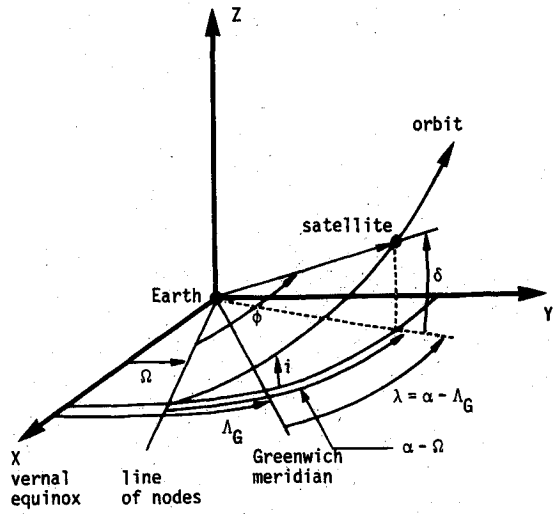

Fig. 2 Geometry of geographical latitude δ and longitude λ.

With these definitions, one can finally express the secular part of Eq. (29) symbolically as

$$\langle \cdots \rangle = \sum_{p=0}^{\ell} \left[H_{\ell m p} \begin{Bmatrix} \langle C_{\ell m p} \rangle \\ \langle S_{\ell m p} \rangle \end{Bmatrix} + K_{\ell m p} \begin{Bmatrix} \langle -S_{\ell m p} \rangle \\ \langle C_{\ell m p} \rangle \end{Bmatrix} \right] \quad \text{for } (\ell - m) = \begin{Bmatrix} \text{even} \\ \text{odd} \end{Bmatrix} \tag{33}$$

The secular parts of the functions defined in Eqs. (31) have been determined by Poisson series processing using the series developments of cos$L$ and sin$L$ in terms Λ. The nonvanishing terms are summarized in Table 2. It can be seen that the J_{22} term is clearly dominant, followed successively by J_{31}, J_{33}, J_{42}, and J_{44}, i.e., the coefficients with an even difference between the indicies ℓ and m. Remaining tesserals like J_{32}, J_{41}, etc., are less important for near-circular orbits as can be seen in Tables 1 and 2.

Finally, the resulting secular part of the tesseral disturbing function up to ϵ_{42} terms becomes

$$\begin{aligned} R_{\text{tess}} = {} & \epsilon_{22}(1+\sigma)^{-3}\{(1-5e^2/2)H_{220} + 9[(f^2-g^2)H_{221} \\ & + 2fgK_{221}]/4\} + \epsilon_{31}(1+\sigma)^{-4}\{(1+2e^2)H_{311} \\ & + (f^2-g^2)(H_{310}+11H_{312})/8 - fg(K_{310}-11K_{312})/4\} \\ & + \epsilon_{32}(1+\sigma)^{-4}\{f(K_{320}-3K_{321}) - g(H_{320}+3H_{321})\} \\ & + \epsilon_{33}(1+\sigma)^{-4}H_{330} \\ & - \epsilon_{41}(1+\sigma)^{-5}\{f(K_{411}-5K_{412}) + g(H_{411}+5H_{412})\}/2 \\ & + \epsilon_{33}(1+\sigma)^{-4}H_{330} + \epsilon_{42}(1+\sigma)^{-5}H_{42i} \end{aligned} \tag{34}$$

Terms of order $\epsilon_{22}e^3$, $\epsilon_{33}e^2$, ϵ_{43}, and ϵ_{44} as well as higher harmonics have been neglected here.

The derivatives of the tesseral disturbing function with respect to the selected elements can be derived from Eq. (34).[14] The derivative with respect to ψ requires some care. The angle ψ occurs only in trigonometric arguments as part of χ [cf. Eq. (6) and Appendix], so that $\partial R/\partial\psi = \partial R/\partial\chi = m\partial R/\partial\gamma_{\ell m}$.

Solar Radiation Pressure Perturbations

Solar radiation pressure perturbations result from the impingement of photons on the satellite surface. The perturbing acceleration induced by solar radiation pressure depends on satellite properties such as the projected area/mass ratio and reflectivity parameters.[17] For the purposes here, constant values are taken throughout since variations with time are highly satellite dependent (e.g., attitude evolution). The solar radiation induced acceleration can be expressed as

$$-2\tau S'(A/m)(a'/r')^2 u' \tag{35}$$

where the prime refers to the sun only. The reflectivity parameter τ is at most equal to 1 (for complete specular reflection). It is seen in Eq. (35) that the force varies inversely in proportion to the square of the distance from the sun and is taken to be directed along the Earth-sun line. The small variations in the force due to the satellite's relative position to the Earth are ignored: these can be shown to be less than the natural variations in the solar constant itself. On the other hand, seasonal variations in the radiation intensity due to the Earth's orbit eccentricity are accounted for. Shadowing effects occur during the eclipse seasons of about 45 days around the equinoxes with a maximum duration of about 70 min. These effects are neglected here.

The acceleration in Eq. (35) can be expressed as the gradient of the solar radiation disturbing function

$$R_{SR} = -2\tau S'(A/m)(a'/r')^2(u'\cdot r) \tag{36}$$

In terms of the adopted nonsingular elements and in units of radians/day, one obtains:

$$\bar{R}_{SR} = -\epsilon_{SR}(a'/r')^2(1+\sigma)\langle (r/a)(u\cdot u')\rangle \tag{37}$$

with

$$\epsilon_{SR} = \frac{86400}{n_s r_s} 2\tau S'\left(\frac{A}{m}\right) = 2.535\times 10^{-4}\left(\frac{\tau A}{m}\right) \tag{38}$$

The secular part can explicitly be determined with the aid of Poisson series manipulation of the series for u and r/a, which yields the result

$$R_{SR} = (3/2)\epsilon_{SR}(a'/r')^2(1+\sigma)(fC+gS) \tag{39}$$

Terms of order $\epsilon_{SR}e^3$ have been neglected here. The derivatives of the disturbing function can now be calculated without difficulty.[14]

Application to GEOS-2 Orbit Evolution

After successful completion of its mission, ESA's scientific satellite GEOS-2 was raised out of its geostationary orbit to an almost circular orbit about 260 km higher.[10] At this altitude, the satellite is drifting in a westward direction relative to the rotating Earth with a circulation period of 108 days.

The new GEOS-2 orbit presents an interesting test case for the approximate model for the near-geostationary orbits presented here. Therefore, a numerical integration with one-day stepsize of the averaged equations was performed using an Adams-Bashforth eighth-order prediction-corrector method with Runge-Kutta starter. Initial conditions and reference values for comparison were established by averaging 48 half-hourly values of the orbital elements produced by a different orbit generator containing all short-periodic contributions.

Table 2 Nonvanishing secular parts of $C_{\ell mp}$ and $S_{\ell mp}$ up to second order in eccentricity

ℓ	m	p	$\langle C_{\ell mp}\rangle$	$\langle S_{\ell mp}\rangle$
2	2	0	$1-5e^2/2$	0
2	2	1	$9(f^2-g^2)/4$	$-9fg/2$
3	1	0	$(f^2-g^2)/8$	$fg/4$
3	1	1	$1+2e^2$	0
3	1	2	$11(f^2-g^2)/8$	$-11fg/4$
3	2	0	$-f$	$-g$
3	2	1	$3f$	$-3g$
3	3	0	$1-6e^2$	0
3	3	1	$53(f^2-g^2)/8$	$-53fg/4$
4	1	1	$-f/2$	$-g/2$
4	1	2	$5f/2$	$-5g/2$
4	2	0	$(f^2-g^2)/2$	fg
4	2	1	$1+e^2$	0
4	2	2	$5(f^2-g^2)$	$-10fg$
4	3	0	$-3f/2$	$-3g/2$
4	3	1	$9f/2$	$-9g/2$
4	4	0	$1-11e^2$	0
4	4	1	$53(f^2-g^2)/4$	$-53fg/2$

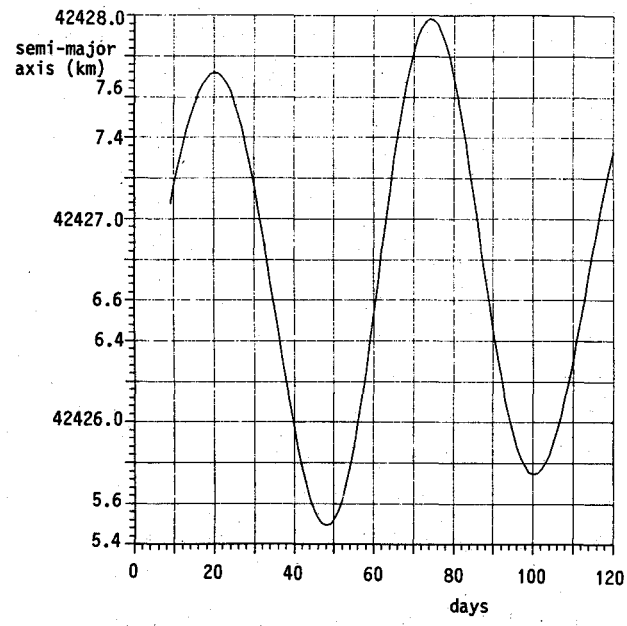

Fig. 3 Semimajor axis prediction over about one circulation period.

Results of Averaged-Orbit Model

The long-term evolutions of eccentricity and polar vectors are essentially identical to those at geostationary altitude. Therefore, attention will be focused on semimajor axis and longitude drift behavior for circulatory conditions. it must be pointed out that the intermediate-period (i.e., about one month) lunar effects on the semimajor axis are absent in the averaged result. This leads to a maximum error of less than 150 m over a two-year period. The nature of the averaging operation, in particular the fact that the moon's position is kept constant during one satellite orbit, is responsible for this error.

Figures 3 and 4 show the resulting behavior of the GEOS-2 semimajor axis and drift rate over a little more than one circulation period. As arbitrary initial epoch, June 3, 1984, was selected. Variations from one circulation period to the next are insignificant on the scale of Figs. 3 and 4, which may thus be considered as characteristic for the long-term motion.

Table 3 Two-year comparison of averaged and short-period orbit models

Parameter	Maximum absolute deviation	Short-period amplitudes
Semimajor axis, m	147	~1000
Eccentricity	6×10^{-6}	$\sim10^{-4}$
Argument of perigee, deg	1.4	~2
Inclination, deg	8×10^{-3}	–
Longitude of nodes, deg	0.04	–
Geographical longitude, deg	0.35	–
Drift rate, deg/day	4×10^{-3}	$\sim10^{-2}$

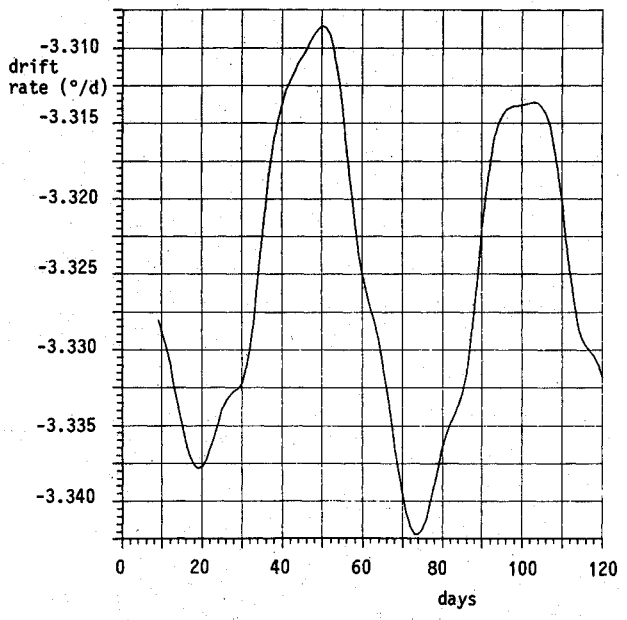

Fig. 4 Drift rate prediction over about one circular period.

In order to assess the accuracy of the averaged orbit model, a comparison with the numerical results based on the short-periodic variations was performed over an interval of two years. Table 3 summarizes the results of the evaluation. The savings in computing time are substantial, as the averaged orbit model requires only about 5% of the time required by the short-period orbit generator.

Approximate Analytical Model

A simple model for the long-term semimajor axis and drift evolution can be derived from the theory outlined above.

For near-circular, near-equatorial orbits, the $\dot{\psi}$ term in the drift equation [cf., Eqs. (5), (6), and (8)] may be approximated as:

$$\dot{\psi}\cong-(2/c_\sigma)R_\sigma \tag{40}$$

The dominant perturbing influences on this part of the drift rate are due to Earth's oblateness and lunisolar effects. Using the disturbing function in Eqs. (10) and (22) with the subsequent expressions for the secular terms, one obtains

$$\dot{\psi}\cong3\epsilon_2c_\sigma^7-\Sigma\epsilon'\{3(C^2+S^2)-2\}/c_\sigma^3 \tag{41}$$

where the summation refers to the contributions of the sun and moon. It can be shown that the parallactic terms are not significant relative to the approximations to be made here.

Since the attention is focused on deriving a representative long-term drift behavior, the C^2+S^2 term in Eqs. (41) will be replaced by its mean value over the respective third-body revolution. Taking both the sun and moon in circular orbits in the ecliptic, one can simplify as

$$\langle C^2+S^2\rangle\cong\langle1-(u_3')^2\rangle=1-0.5\sin^2(23.44\text{ deg})=0.9209 \tag{42}$$

Substituting the known constants into Eqs. (41), one obtains the following approximation for the long-term drift rate:

$$\langle\dot{\psi}\rangle=\{26.83c_\sigma^7-6.52/c_\sigma^3\}\times10^{-3}\text{ deg/day} \tag{43}$$

After evaluation of c_σ from initial or mean values, a representative constant drift rate is established.

When the semimajor axis is taken equal to r_s so that $c_\sigma=1$, one finds $\dot{\psi}_s=2.03\times10^{-2}$ deg/day, which in this particular case is identical to the total drift rate, cf. Eq. (5). This result may be used to calculate an approximate value for the "perturbed" geostationary semimajor axis a_g, cf. Eq. (5),

$$a_g\cong r_s\{1+2\dot{\psi}_s/(3n_s)\}=r_s+1.58=42165.78\text{ km} \tag{44}$$

In the case of GEOS-2, one has $c_\sigma=0.9969$ (cf. Fig. 3), which leads to $\langle\dot{\psi}\rangle=1.97\times10^{-2}$ deg/day. Numerical integration of the complete long-term ψ equation confirms this result to within 0.5 deg over a 1000 day period. This would appear to endorse the validity of the various approximations performed before arriving at this result.

Differentiation of the drift equation (5) leads to

$$\ddot{\chi}=-1.5\tilde{n}_sc_\sigma^5\dot{\sigma} \tag{45}$$

where $\tilde{n}_s$ incorporates the offset in the drift rate induced by the dominant perturbing effects,

$$\tilde{n}_s=n_s\{1+(173.4c_\sigma^4+18.1/c_\sigma^6)\times10^{-6}\} \tag{46}$$

An explicit result for $\dot{\sigma}$ that is essentially only affected by tesseral harmonics follows from Eqs. (8) and (34),

$$\dot{\sigma}\cong-4\epsilon_{22}c_\sigma^5K_{220}-2\epsilon_{31}c_\sigma^7K_{311} \tag{47}$$

where a near-equatorial orbit has been considered. Combination with Eq. (45) gives $\ddot{\chi}=f(\chi)$ with f defined as

$$f(\chi)=18\epsilon_{22}\tilde{n}_sc_\sigma^{10}\sin\gamma_{22}-4.5\epsilon_{31}\tilde{n}_sc_\sigma^{12}\sin\gamma_{31} \tag{48}$$

For initial conditions in the circulation domain, $\dot{\chi}_0$ is large with respect to the drift rate variations induced by the perturbing forces (for GEOS-2 by a factor 120, cf. Fig. 4). Thus, it appears justified to integrate $\ddot{\chi}=f(\chi)$ in the following manner:

$$\dot{\chi}(\chi)=\left\{\dot{\chi}_0^2+2\int_{\chi_0}^{\chi}f(\xi)\mathrm{d}\xi\right\}^{1/2}\cong\dot{\chi}_0+\frac{1}{\dot{\chi}_0}\int_{\chi_0}^{\chi}f(\xi)\mathrm{d}\xi$$

$$=\dot{\chi}_0-9c_\sigma^{10}(\tilde{n}_s/\dot{\chi}_0)[\epsilon_{22}\cos\gamma_{22}-0.5\epsilon_{31}c_\sigma^2\cos\gamma_{31}]_{\chi_0}^{\chi} \tag{49}$$

The satellite longitude position may now be approximated as a linear function of time with a rate given by the averaged (over χ) value of Eq. (49),

$$\langle\dot{\chi}\rangle\cong\dot{\chi}_0+9c_\sigma^{10}(01s/\dot{\chi}_0)\{\epsilon_{22}\cos2(\chi_0-\lambda_{22})$$

$$-0.5\epsilon_{31}c_\sigma^2\cos(\chi_0-\lambda_{31})\} \tag{50}$$

For GEOS-2, one finds a mean drift rate of -3.3247 deg/day, which results in a maximum longitude error of less than 0.5 deg over a two-year period.

Finally, a simple approximation for the long-term semimajor axis evolution is obtained from Eq. (49) when using the drift equation of Eq. (5) and the constant approximation for $\dot{\psi}$ in Eq. (43),

$$\sigma(\chi)=\{1+(\dot{\chi}-\langle\dot{\psi}\rangle)/n_s\}^{-2/3}-1 \tag{51}$$

In the GEOS-2 case, this prediction leads to a maximum error of 165 m with respect to the results from the short-period model over the two years considered.

Conclusion

An averaged-orbit model for describing the long-term evolution of near-geostationary satellite orbits has been presented. The results have been illustrated using the actual GEOS-2 orbit, which is about 260 km above geostationary altitude. The accuracies of eccentricity and polar vector predictions have been excellent in comparison to reference values obtained from a different orbit generator containing all short-periodic terms. Semimajor axis and longitude predictions have errors below 150 m and 0.4 deg, respectively, uniformly over a two-year interval. In addition, a simple analytical model for semimajor axis and longitude drift evolutions has been derived from the general theory. This model has only slightly degraded accuracies compared to the numerically evaluated averaged model. The long-term valid orbit model presented should be useful for quick orbit predictions, in particular in the case of satellites that have been removed from the geostationary orbit.

Appendix: Nonsingular Inclination Functions

The nonsingular representations of Kaula's inclination functions[16] are summarized below as far as they are needed in the final averaged tesseral disturbing function in Eq. (34).

$\ell,m=2,2$:

$$\begin{pmatrix} H_{220} \\ K_{220} \end{pmatrix} = \frac{3}{X^2}\begin{pmatrix} \cos\gamma_{22} \\ \sin\gamma_{22} \end{pmatrix}$$

$$\begin{pmatrix} H_{221} \\ K_{221} \end{pmatrix} = \frac{6}{X^2}\left[(h^2-k^2)\begin{pmatrix} \cos\gamma_{22} \\ \sin\gamma_{22} \end{pmatrix} + 2hk\begin{pmatrix} -\sin\gamma_{22} \\ \cos\gamma_{22} \end{pmatrix}\right]$$

$\ell,m=3,1$:

$$\begin{pmatrix} H_{310} \\ K_{310} \end{pmatrix} = -\frac{15}{2X^3}\left[(h^2-k^2)\begin{pmatrix} \cos\gamma_{31} \\ \sin\gamma_{31} \end{pmatrix} - 2hk\begin{pmatrix} -\sin\gamma_{31} \\ \cos\gamma_{31} \end{pmatrix}\right]$$

$$\begin{pmatrix} H_{311} \\ K_{311} \end{pmatrix} = -\frac{3}{2X}\left(6-\frac{20}{X}+\frac{15}{X^2}\right)\begin{pmatrix} \cos\gamma_{31} \\ \sin\gamma_{31} \end{pmatrix}$$

$$\begin{pmatrix} H_{312} \\ K_{312} \end{pmatrix} = -\frac{3}{2X}\left(1-\frac{10}{X}+\frac{15}{X^2}\right)\left\{(h^2-k^2)\begin{pmatrix} \cos\gamma_{31} \\ \sin\gamma_{31} \end{pmatrix} + 2hk\begin{pmatrix} -\sin\gamma_{31} \\ \cos\gamma_{31} \end{pmatrix}\right\}$$

$\ell,m=3,2$:

$$\begin{pmatrix} H_{320} \\ K_{320} \end{pmatrix} = \frac{15}{X^3}\left[h\begin{pmatrix} \cos\gamma_{32} \\ \sin\gamma_{32} \end{pmatrix} - k\begin{pmatrix} -\sin\gamma_{32} \\ \cos\gamma_{32} \end{pmatrix}\right]$$

$$\begin{pmatrix} H_{321} \\ K_{321} \end{pmatrix} = \frac{15}{X^2}\left(2-\frac{3}{X}\right)\left[h\begin{pmatrix} \cos\gamma_{32} \\ \sin\gamma_{32} \end{pmatrix} + k\begin{pmatrix} -\sin\gamma_{32} \\ \cos\gamma_{32} \end{pmatrix}\right]$$

$\ell,m=3,3$:

$$\begin{pmatrix} H_{330} \\ K_{330} \end{pmatrix} = \frac{15}{X^3}\begin{pmatrix} \cos\gamma_{33} \\ \sin\gamma_{33} \end{pmatrix}$$

$\ell,m=4,1$:

$$\begin{pmatrix} H_{411} \\ K_{411} \end{pmatrix} = -\frac{5}{2X^2}\left(37-\frac{35}{X}+\frac{28}{X^2}\right)\left[h\begin{pmatrix} \cos\gamma_{41} \\ \sin\gamma_{41} \end{pmatrix} - k\begin{pmatrix} -\sin\gamma_{41} \\ \cos\gamma_{41} \end{pmatrix}\right]$$

$$\begin{pmatrix} H_{412} \\ K_{412} \end{pmatrix} = -\frac{15}{2X}\left(1-\frac{9}{X}+\frac{21}{X^2}-\frac{14}{X^3}\right)\left[h\begin{pmatrix} \cos\gamma_{41} \\ \sin\gamma_{41} \end{pmatrix} + k\begin{pmatrix} -\sin\gamma_{41} \\ \cos\gamma_{41} \end{pmatrix}\right]$$

$\ell,m=4,2$:

$$\begin{pmatrix} H_{421} \\ K_{421} \end{pmatrix} = -\frac{15}{2X^2}\left(15-\frac{42}{X}+\frac{28}{X^2}\right)\begin{pmatrix} \cos\gamma_{42} \\ \sin\gamma_{42} \end{pmatrix}$$

The angle $\gamma_{\ell m}$ appearing here is defined as

$$\gamma_{\ell m} = m(\chi+\lambda_s-\lambda_{\ell m}), \quad \ell=2,3,..; \quad m=2,...,\ell \qquad \text{(A2)}$$

Note that the angle $\chi+\lambda_s-\lambda_{\ell m}$ designates the angular distance between the satellite's longitudinal position and the reference longitude $\lambda_{\ell m}$ belonging to the $J_{\ell m}$ tesseral harmonic.

Acknowledgment

The author is grateful to Mr. S. Pallaschke for providing the reference values obtained from the short-period orbit generator.

References

[1]Allen, R.R. and Cooke, G.E., "The Long-Period Motion of the Plane of a Distant Circular Orbit," *Proceedings of the Royal Society of London,* Ser. A, Vol. 280, 1964, pp. 97-109.

[2]Allen, R.R., "Perturbations of a Geostationary Satellite by the Longitude-Dependent Terms in the Earth's Gravitational Field," *Planetary Space Sciences,* Vol. 11, 1963, pp. 1325-1334.

[3]Blitzer, L., "Satellite Resonances and Librations Associated with Tesseral Harmonics of the Geopotential," *Journal of Geophysical Research,* Vol. 71, 1966, pp. 3557-3665.

[4]Flury, W., "Perturbation Theory for Geostationary Satellites: Application of the Bohlin-von Zeipel Method," *Proceedings of 10th International Symposium on Space Technology and Science,* AGNE Publishing, Tokyo, 1973, pp. 365-374.

[5]Graf, O.F. Jr., "Lunar and Solar Perturbations on the Orbit of a Geosynchronous Satellite," Paper AAS-75-023, presented at *AAS/AIAA Astrodynamics Conference,* Nassau, Bahamas, 1975.

[6]Richardson, D.L., "The Long-Period Motion of 24-Hour Satellites," AIAA Paper 76-828, 1976.

[7]Kamel, A.A., "Geosynchronous Satellite Ephemeris Due to Earth's Triaxiality and Luni-Solar Effects," *Journal of Guidance, Control, and Dynamics,* Vol. 5, March-April 1982, pp. 189-193.

[8]Soop, E.M., "Introduction to Geostationary Orbits," European Space Agency, Paris, France, ESA-SP-1053, Nov. 1983.

[9]Hechler, M. and Van der Ha, J.C., "Probability of Collisions in the Geostationary Ring," *Journal of Spacecraft and Rockets,* Vol. 18, July-Aug. 1981, pp. 361-366.

[10]Beech, P., Soop, M., and Van der Ha, J., "The De-Orbiting of GEOS-2," *ESA Bulletin,* No. 38, May 1984, pp. 86-89.

[11]Broucke, R.A., "A Fortran-4 System for the Manipulation of Symbolic Poisson Series with Applications to Celestial Mechanics," *Institute for Advanced Study in Orbital Mechanics,* University of Texas, Austin, Paper IASOM-TR-80-3, 1980.

[12]Broucke, R.A. and Cefola, P.J., "On the Equinoctial Orbit Elements," *Celestial Mechanics,* Vol. 5, 1972, pp. 303-310.

[13]Fitzpatrick, P.M., *Principles of Celestial Mechanics,* Academic Press, New York, 1970, Chap. 8.2.

[14]Van der Ha, J.C., "Very Long-Term Orbit Evolution of a Geostationary Satellite," MAO Working Paper 122, European Space Operations Centre, Darmstadt, FRG, March 1980.

[15]Wagner, C.A., Lerch, F.J., Brown, J.E., and Richardson, J.A., "Improvement in the Geopotential Derived from Satellite and Surface Data (GEM 7 and 8)," *Journal of Geophysical Research,* Vol. 82, 1977, pp. 901-914.

[16]Kaula, W.M., *Theory of Satellite Geodesy,* Blaisdell Publishing Co., Waltham, MA, 1966.

[17]Van der Ha, J.C. and Modi, V.J., "Analytical Evaluation of Solar Radiation Induced Orbital Perturbations of Space Structures," *Journal of the Astronautical Sciences,* Vol. 25, 1977, pp. 283-306.